Available online at www.sciencedirect.com
SCIENCE DIRECT
Catalysis Today 107–108 (2005) 330–337
CATALYSIS TODAY
www.elsevier.com/locate/cattod

Effect of the Pt/Co ratio upon the catalytic behavior of PtCoFerrierite washcoated on cordierite monoliths

Alicia V. Boix, Eduardo A. Lombardo, Eduardo E. Miró *

Instituto de Investigaciones en Catálisis y Petroquímica, INCAPE (FIQ, UNL-CONICET). Santiago del Estero 2829, 3000 Santa Fe, Argentina

Available online 15 August 2005

Abstract

CoFER and PtCoFER were prepared with different Co loadings and Co/Pt ratios. The resulting powders were washcoated on ceramic honeycombs. To increase adherence, silica was added to the slurry as a binder. The samples were assayed for the SCR of NO_x with methane in excess oxygen. The maximum conversion of NO_x to N_2 for each formulation when plotted versus either Co loading or Co/Pt ratio presented maxima. All catalysts partially deactivated with 2% water. A thorough TPR, XPS and LRS characterization of fresh and deactivated catalysts showed that two deactivation mechanisms are operative. At low Co loadings, the formation of Pt clusters is responsible for the low selectivity, while for higher loadings Co_3O_4 is formed and is the non-selective species.

Keywords: CoPtFerrierite; Cordierite monoliths; NO_x reduction; Deactivation

1. Introduction

Interest in the use of metal-exchanged zeolites for the abatement of atmospheric pollutants has increased in the last few years [1]. The selective reduction of NO_x in stationary sources using ammonia as reductant is an example of a well-established technology for which metal–zeolites can be applied [2,3]. However, ammonia is a toxic, corrosive gas and its use is a serious drawback in the implementation of this approach. On the other hand, methane, a more friendly reductant, has been the subject of a great research effort in the last decade [4,5]. Environmental applications such as hydrocarbon adsorption for the cold start of Otto cycle engines and NO_x reduction in lean conditions for both diesel and Otto engine exhausts are also other examples of emerging technologies [1].

Concerning the selective reduction of NO_x with methane under excess oxygen, the main disadvantage of metal–zeolites is their low hydrothermal stability. Co, In and Pd ions exchanged in ZSM5, mordenite and ferrierite are active and selective catalysts under dry conditions. However, under realistic conditions, when ca. 10% water is present in the feed, all these catalysts suffer deactivation. Kikuchi et al. [6,7] reported that the addition of noble metals (Pt, Rh and Ir) to InHZSM5 results in a better water tolerance, suggesting that the role of the precious metal is to accelerate NO oxidation and NO_2 adsorption capacity even in the presence of water. Both these authors [8] and Montes and co-workers [9] found a similar effect in PdCo-containing zeolites.

It is known that in order to use the systems under study in combustion exhausts, the zeolite particles have to be shaped as monoliths in either of these three ways: massive extrudated zeolite monoliths [10], zeolite films grown on top of ceramic or metallic substrates [11,12] and zeolite powder washcoated on cordierite [13,14]. Our group has undertaken a systematic study of the washcoating conditions for ZSM5, mordenite and ferrierite [15]. We have found that the slurry concentration and the number of immersions can be adequately combined to obtain different coating thickness and geometry. We have also found that the washcoat adherence increases with the decrease in the size of the crystals aggregates deposited on the monolith, and that the addition of SiO_2 as a binder enhances the adherence of the three zeolites under study, probably due to an improvement in the interparticle adhesion.

* Corresponding author.
E-mail address: emiro@fiqus.unl.edu.ar (E.E. Miró).

0920-5861/$ – see front matter © 2005 Elsevier B.V. All rights reserved.
doi:10.1016/j.cattod.2005.07.082

In the same vein, and for PtCoFerrierite washcoated monoliths [16], we reported that SiO_2 not only improves the mechanical stability but also helps to obtain a selective catalyst. We suggested that this phenomenon is due to the fact that the small SiO_2 particles impair the formation of Pt and Co_3O_4 clusters on the zeolite crystals outer surface. It is known that these clusters are highly active in deep methane oxidation, thus consuming the reductant and decreasing the selectivity towards NO_x reduction.

In the present work, we study the effect of the Pt/Co ratio upon the catalytic performance and the physicochemical characteristics of PtCoFerrierite washcoated on cordierite honeycombs. The main objective of our research is to contribute to a deeper understanding of the nature of active sites and deactivation processes through a detailed LRS, XPS, SEM and TPR characterization.

2. Experimental

2.1. Preparation of Co and PtCoFerrierite unsupported catalysts

Catalysts were prepared by ion exchange starting from KFerrierite of unit cell composition, $[Na, K)_{3.7}(AlO_2)_{3.7}$-$(SiO_2)_{23.3}\cdot 10\ H_2O$. The cobalt-exchanged KFerrierite (CoFER) solids were prepared using a cobalt acetate solution (0.025 M), with a ratio of 10 g zeolite in 1.5 L solution.

In order to analyze the effect of the Co load and the Co/Pt ratio incorporated to the catalyst, solids with different cobalt content were prepared at the following exchange temperatures: 298, 323 and 353 K. The exchange time was 24 h after which the solids were filtered, washed and dried at 393 K for 8 h. CoFER was calcined, heated at 2 K/min in O_2 flow up to 623 K, and kept at this temperature for 2 h. The PtCoFER catalysts were obtained by performing a second exchange in the CoFER samples, at room temperature, with $Pt(NH_3)_4(NO_3)_2$. About 0.5% (w/w) Pt was incorporated to the solid. The bimetallic samples were calcined in O_2 at a slow heating rate (0.5 K/min, up to 623 K). The catalysts obtained are shown in Table 1.

2.2. Preparation of washcoated monolithic catalysts

2.2.1. Washcoat of CoFerrierite

A suspension with 40% (w/w) of CoFER (in deionized water) was used to impregnate a cordierite support (Corning) having square-section cells with a density of 400 cells/(in.)^2. Three successive immersions of the monolith in the suspension were performed to achieve the expected zeolite load (approximately 20%, w/w, on a dry basis). After each immersion, air was softly blown to eliminate the excess suspension to achieve a homogeneous film on the ceramic surface. It was dried at 393 K for 12 h and then calcined in oxygen flow at 823 K for 2 h.

2.2.2. Washcoat of PtCoFerrierite

Using the PtCoFER powder, the monolith impregnation was done following a sequence similar to that of the former preparation (Section 2.2.1). It was performed with or without the addition of a binder (cab-o-sil, surface area = 200 m^2/g; particle diameter = 5–30 nm). The washcoated monolith was calcined heating at 0.5 K/min in O_2 flow up to 823 K and kept there for 2 h in order to obtain a good adherence of the zeolite crystals to the monolith walls.

2.3. Catalytic measurements

Mono and bimetallic powder catalysts and those supported on the ceramic monolith were evaluated in a continuous flow system. Prior to the catalytic evaluation, the monometallic samples were only calcined in O_2 flow at 823 K while the bimetallic solids were first calcined in O_2 at 823 K and then reduced in H_2 at 623 K. The typical composition of the reacting stream was the following: 1000 ppm NO, 1000 ppm CH_4, 2% O_2, in helium. The reaction was performed under

Table 1
Catalytic performance of the solids studied

Catalysts[a]	Co exchange temperature (K)[b]	Co/Pt	%Conversion[c], 0% H_2O			%Conversion[c], 2% H_2O		
			NO to N_2	CH_4	T_{max}[d]	NO to N_2	CH_4	T_{max}[d]
$Co_{4.3}$FER[b]	353	–	17	90	773	7	95	773
$PtCo_{4.3}$FER		30	45	90	773	28	70	823
$PtCo_{4.3}$FER-M		30	41	82	773	25	70	823
$Co_{3.4}$FER	323	–	12	95	823	5	95	823
$PtCo_{3.4}$FER		22	22	80	723	15	95	723
$PtCo_{3.4}$FER-M		22	28	98	748	20	65	723
$Co_{1.2}$FER	298	–	38	80	773	15	55	773
$PtCo_{1.2}$FER		9.7	22	70	723	9	50	773
$PtCo_{1.2}$FER-M		9.7	25	70	748	12	60	773

[a] All the catalysts were calcined at 623 K. The PtCoFER solids were reduced in situ at 623 K before reaction. The subscript shows the cobalt exchanged % (%, w/w).
[b] Exchange solution: 0.025 M Co $(CH_3COO)_2$, 10 g KFER/1.5 L of solution.
[c] Reaction conditions: 1000 ppm NO, 1000 ppm CH_4, 2% O_2 in He, GHSV = 20,000 h^{-1}.
[d] Temperature of the maximum NO to N_2 conversion.

atmospheric pressure at temperatures between 523 and 923 K, with space velocity (GHSV) = 20,000 h^{-1}. The washcoated monoliths (1 cm × 1 cm × 2 cm) were placed in the same reactor between two quartz wool plugs. In some runs, water was also introduced in the feed in order to test the deactivation behavior of the best formulations.

The gaseous mixtures were analyzed with an SRI 9300B chromatograph equipped with a 5 Å molecular sieve column. The NO_x conversion (C_{NO}, %) was calculated from N_2 production: $C_{NO} = 2 \times 100 \times ([N_2]/[NO]^\circ)$, where $[NO]^\circ$ is the NO initial concentration. The CH_4 conversion (C_{CH_4}, %) was obtained as $C_{CH_4} = 100 \times ([CH_4]^0 - [CH_4])/[CH_4]^0$.

2.4. TPR experiments

These experiments were performed using an Okhura TP-2002 S instrument equipped with a TCD detector. The reducing gas was 5% H_2 in Ar, flowing at 30 mL/min and the heating rate was 10 K/min up to 1173 K. 0.050 g of the fresh powder samples, Co and PtCoFER, were pre-treated in situ in flowing O_2, heating at 2 K/min up to 623 K and kept at that temperature for 2 h.

2.5. Raman spectroscopy

The Raman spectra were recorded with a TRS-600-SZ-P Jasco Laser Raman instrument, equipped with a change-coupled device (CCD) with the detector cooled to about 153 K using liquid N_2. The excitation source was the 514.5-nm line of a Spectra 9000 Photometrics Ar ion laser. The laser power was set at 30 mW. For Raman spectroscopy the powder sample, calcined and used, was pressed at 4 bar into self-supporting wafers and the monolith samples were used as they had been prepared and after use in the catalytic test.

2.6. Surface analysis by XPS

X-ray photoelectron spectra were acquired with a Shimadzu Model ESCA 750 electron spectrometer equipped with an Al Kα X-ray source ($h\nu$ = 1486.6 eV). The Si 2p, Al 2p, Pt 4f, Co 2p, O 1s, K 2p, Al 2s and C 1 s core-level spectra were recorded for all the samples. For the Al 2p and Pt 4f signals the situation was more complex because they overlapped. In order to analyze the contribution of the two elements, it was assumed that the spin-orbit splitting for Pt was fixed at 3.35 eV and the Pt $4f_{5/2}$/Pt $4f_{7/2}$ intensity ratio was kept constant (0.75). In the case of Co 2p, the spin-orbit separation was equal to 16 eV and the $2p_{1/2}/2p_{3/2}$ ratio was 0.5. Prior to the XPS measurement, fresh and used samples were dehydrated in the pretreatment chamber (10^{-5} Torr).

2.7. SEM characterization

The samples morphology was also examined with a scanning electron microscope (SEM) Jeol JSM-35C operated at accelerating voltages of 20–25 kV. The solids were glued to the sample holder with silver paint and covered with a thin gold layer to improve the images.

3. Results

Table 1 shows the powder catalysts prepared by successive ion exchange of cobalt and platinum salts at 353, 323 and 298 K. In this way, loads of 4.3, 3.4 and 1.2% (w/w) of cobalt were exchanged in the Kferrierite matrix. To obtain different Co/Pt ratios, approximately 0.5% of Pt was exchanged on the three CoFERs, at room temperature.

The catalytic activity of both monometallic and bimetallic ferrierite is also shown in Table 1. Both CoFER and PtCoFER deactivated when water was added to the feed. With CoFER the best NO to N_2 conversion (38%) was obtained with the lowest Co content, while the PtCoFER with Co/Pt = 30 yielded the highest conversion to N_2 45%. The presence of Pt increased the conversion of NO to N_2 from 17 to 45% when Co/Pt = 30 and from 12 to 22% when Co/Pt = 22. But when the ratio was 9.7, the selectivity decreased. On the other hand, the PtCoFERs with Co/Pt = 30

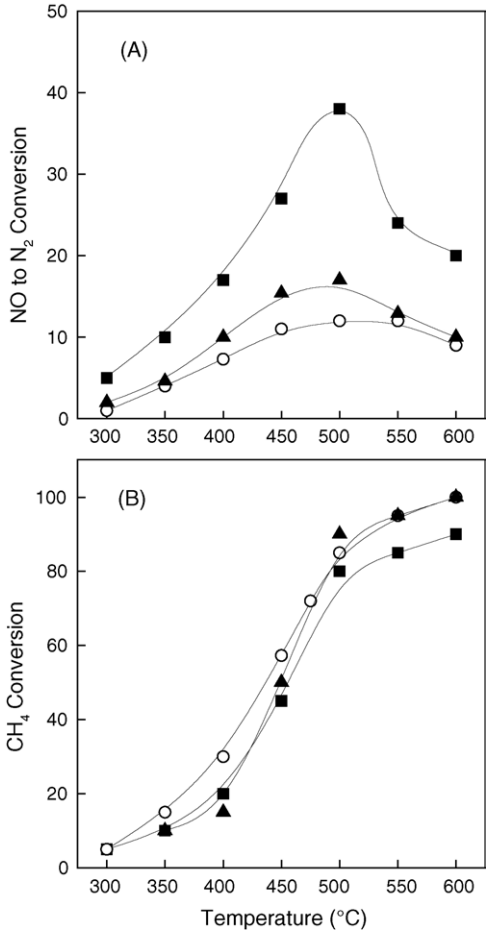

Fig. 1. Catalytic behavior of powder CoFER. Reaction conditions: 1000 ppm NO, 1000 ppm CH_4, GHSV = 20,000 h^{-1}. (A) NO to N_2 conversion. (B) Methane conversion. (■) $Co_{1.2}$FER, (○) $Co_{3.4}$FER, (▲) $Co_{4.3}$FER.

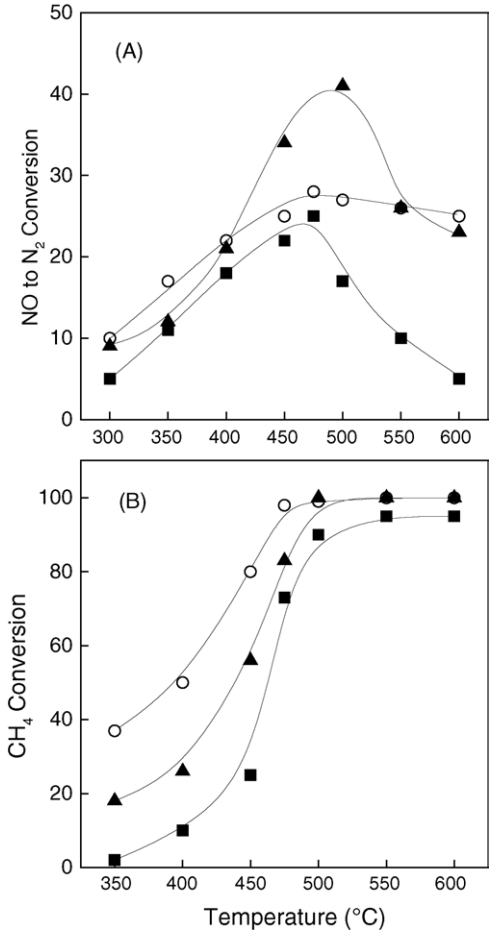

Fig. 2. Catalytic behavior of PtCoFER-M. Reaction conditions: 1000 ppm NO, 1000 ppm CH_4, GHSV = 20,000 h^{-1}. (A) NO to N_2 conversion. (B) Methane conversion. (■) $PtCo_{1.2}FER$, (○) $PtCo_{3.4}FER$, (▲) $PtCo_{4.3}FER$.

and 22 showed an increased resistance to water deactivation, e.g. the monometallic catalysts lost 60% of their activity while the bimetallic ones with Co/Pt ratios of 22 or more, only lost 30–40%. All the monoliths prepared with the addition of SiO_2 showed activities very similar to, or slightly

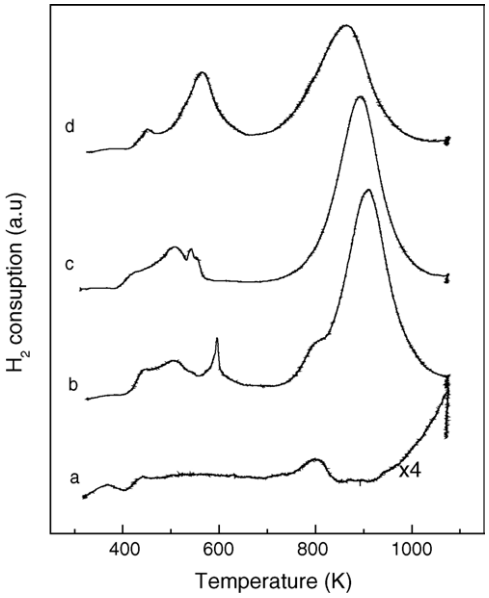

Fig. 3. TPR of CoFER powders, 5% H_2 in Ar. Profiles (a) calcined $Co_{1.2}FER$, (b) calcined $Co_{3.4}FER$, (c) calcined $Co_{4.3}FER$ and (d) used $Co_{4.3}FER$.

higher than, the starting powders. Figs. 1 and 2 display the catalytic activities for CoFER powder and PtCoFER-M at different temperatures, showing the typical behavior in both NO and methane conversions.

The TPR profiles of the unsupported CoFERs are shown in Fig. 1, and the H_2 consumption is shown in Table 2. The $Co_{1.2}FER$ is hardly reducible and only shows a tiny peak at 800 K and the beginning of another at ca. 950 K. When the Co content increases, profiles b and c in Fig. 3 show the presence of two well-defined peaks: (i) cobalt oxides (CoO and/or Co_3O_4) at temperatures between 423 and 623 K and (ii) Co^{2+} at exchange positions, reducible at temperatures higher than 800 K. Note that according to Table 2, not all the cations are reduced in the interval of temperatures explored (300–1073 K). After use in the reactor with a dry feed, the proportion of oxides in the catalysts increased from 18 to 25% (Table 2 and profile d in Fig. 3). The reducibility of the

Table 2
Reducibility of CoFER and PtCoFER powders

Sample	Pretreatment[a,b]	H_2/Co (T_{max})[c]		
$Co_{1.2}FER$	Calculated	–	–	0.11 (805)
	Used	–	–	0.12 (825)
$Co_{3.4}FER$	Calculated	0.13 (505–598)		0.70 (910)
	Used	0.20 (430)		0.67 (900)
$PtCo_{3.4}FER$	Calculated	0.23 (400)		0.60 (720)
	Used	0.26 (423)	0.2 (620)	0.75 (789)
$Co_{4.3}FER$	Calculated	0.18 (507)		0.65 (893)
	Used	0.25 (585)		0.60 (864)
$PtCo_{4.3}FER$	Calculated	0.29 (432)		0.53 (752)
	Used	0.20 (400)	0.28 (600)	0.72 (855)

[a] Prior to TPR, the sample was calcined in situ for 2 h at 623 K.
[b] Prior to TPR, the sample was calcined and reduced at 623 K and then, used in reaction conditions.
[c] Peak maximum temperature.

calcined and used bimetallic samples is shown in Table 2. The samples with Co/Pt = 30 and 22 exhibit similar TPR profiles [16].

The Raman bands of the starting calcined KFER and the catalysts containing 1.2% Co cannot be observed due to the high fluorescence. However, the solids with higher Co content have a very good signal to noise ratios. The Raman spectra of CoFER are shown in Fig. 4A. In the fresh catalyst (spectrum b), two small signals appear at 340 and 690 cm^{-1}, respectively. The former one belongs to the support and the latter to Co_3O_4. In the used catalyst (spectrum a), the characteristic fingerprints of Co_3O_4 become clearly visible. The spectra of $PtCo_{3.4}FER$ at two calcinations temperatures (623 and 823 K) are shown in Fig. 4B. They do not show the bands pertaining to Co_3O_4. Fig. 4C shows the spectra of the $PtCo_{4.3}FER$ with and without the addition of SiO_2 after use. In the latter case (spectrum e), the signal at 690 cm^{-1} has developed.

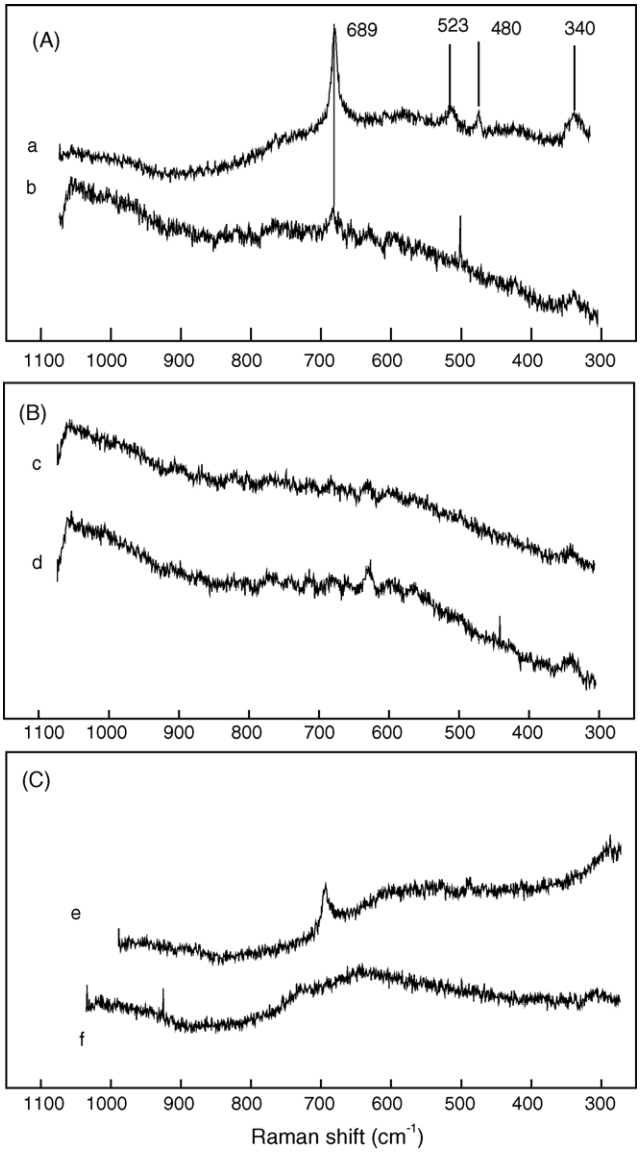

Fig. 4. Laser Raman spectra of CoFER and PtCoFER powders. (a) used CoFER, (b) CoFER calcined at 623 K, (c) PtCoFER + SiO_2 calcined at 823 K, (d) PtCoFER + SiO_2 calcined at 623 K, (e) PtCoFER + SiO_2 calcined at 823 K, reduced at 623 K, after use and (f) PtCoFER calcined at 623 K, reduced at 623 K, after use.

The spectra of $PtCo_{4.3}FER$ washcoated on commercial cordierite together with the spectrum of the naked cordierite are shown in Fig. 5. In the monolith washcoated with S_iO_2 added and calcined at 823 K, two small signals at 630 and 690 cm^{-1} are visible. The latter one belongs to Co_3O_4 while the band at 630 cm^{-1} may correspond to highly dispersed Co_xO_y species [17]. The monolith that remained selective for N_2 production shows the band at 690 cm^{-1} and a second one at 340 cm^{-1} which belongs to the ferrierite structure. On the other hand, the catalysts which were unselective (traces d and e) clearly show the three Raman bands of Co_3O_4.

Table 3 shows the XPS data obtained with bimetallic powder catalysts whose Co/Pt ratios were 30 and 9.7, respectively. The BE values of Co $2p_{3/2}$ correspond to Co^{2+} ions at exchange positions (~782 eV). Platinum exchanged on Coferrierite and calcined-reduced at 623 K after reaction showed Pt $4f_{7/2}$ BEs between 72.7 and 70.8 eV. Vedrine et al. [18] reported similar values for Pt^0 particles of different sizes dispersed in NaY zeolite.

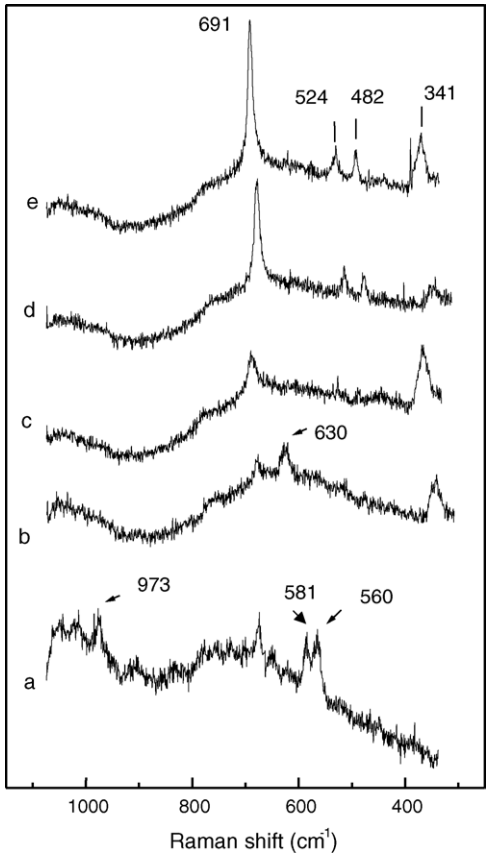

Fig. 5. Laser Raman spectra of (a) cordierite and PtCoFER-M, (b) with SiO_2 and calcined at 823 K, (c) with SiO_2 after use (good N_2 conversion), (d) without SiO_2 after use (low N_2 conversion) and (e) with SiO_2 after 50 h in reaction conditions with 2% water.

Table 3
Surface features of bimetallic powder catalysts

Catalyst	Binding energy (eV)[a] (FWHM)		Surface atomic ratio[b]	
	Co $2p_{3/2}$	Pt $4f_{7/2}$	Co/Si	Pt/Si × 10^3
$PtCo_{4.3}$FER calcined at 623 K	781.8 (3.9)	71.8 (2.2)	0.17	5.0
$PtCo_{4.3}$FER used with 2% H_2O selective to N_2	782.2 (3.9)	71.4 (2.0)	0.16	1.9
$PtCo_{1.2}$FER calcined at 623 K	782.2 (3.7)	72.7 (2.5)	0.84	0.6
$PtCo_{1.2}$FER used with 2% H_2O selective to N_2	782.2 (4.1)	72.6 (2.6)	0.14	1.4
$PtCo_{1.2}$FER used with 10% H_2O no selective	781.5 (4.3)	70.8 (2.1)	0.053	3.0

[a] The binding energies are referenced to the C 1 s peak (284.6 eV).
[b] The surface atomic ratio (Si/Al) varied between 6 and 7.

A relevant piece of information emerges from the surface ratio. For the catalyst with higher Co load ($PtCo_{4.3}$FER), the Co/Si atomic surface ratio remains constant at 0.17 after being on stream for several hours. However, for the catalyst with lower cobalt content the surface cobalt concentration decreases in the used catalyst while the surface is enriched in metallic platinum.

SEM characterization of $PtCo_{3.4}$FER washcoated with SiO_2 as a binder is shown in Fig. 6. Fig. 6a and b show that a homogeneous coating of ca. 30 μm of thickness was obtained. Besides, by comparing the morphology of fresh-calcined and used catalyst (Fig. 6c and d, respectively), a change in the porosity can be observed after reaction. As a matter of fact, while the size of zeolite aggregates does not change, the distance between them is shorter for the used sample.

4. Discussion

The exchange of cobalt in zeolites leads to the formation of different Co species depending on the exchange procedure and on the pretreatments. Cations at exchange positions, Co_3O_4 crystals, highly dispersed non-crystalline cobalt oxide species, and polynuclear Co oxo-ions are

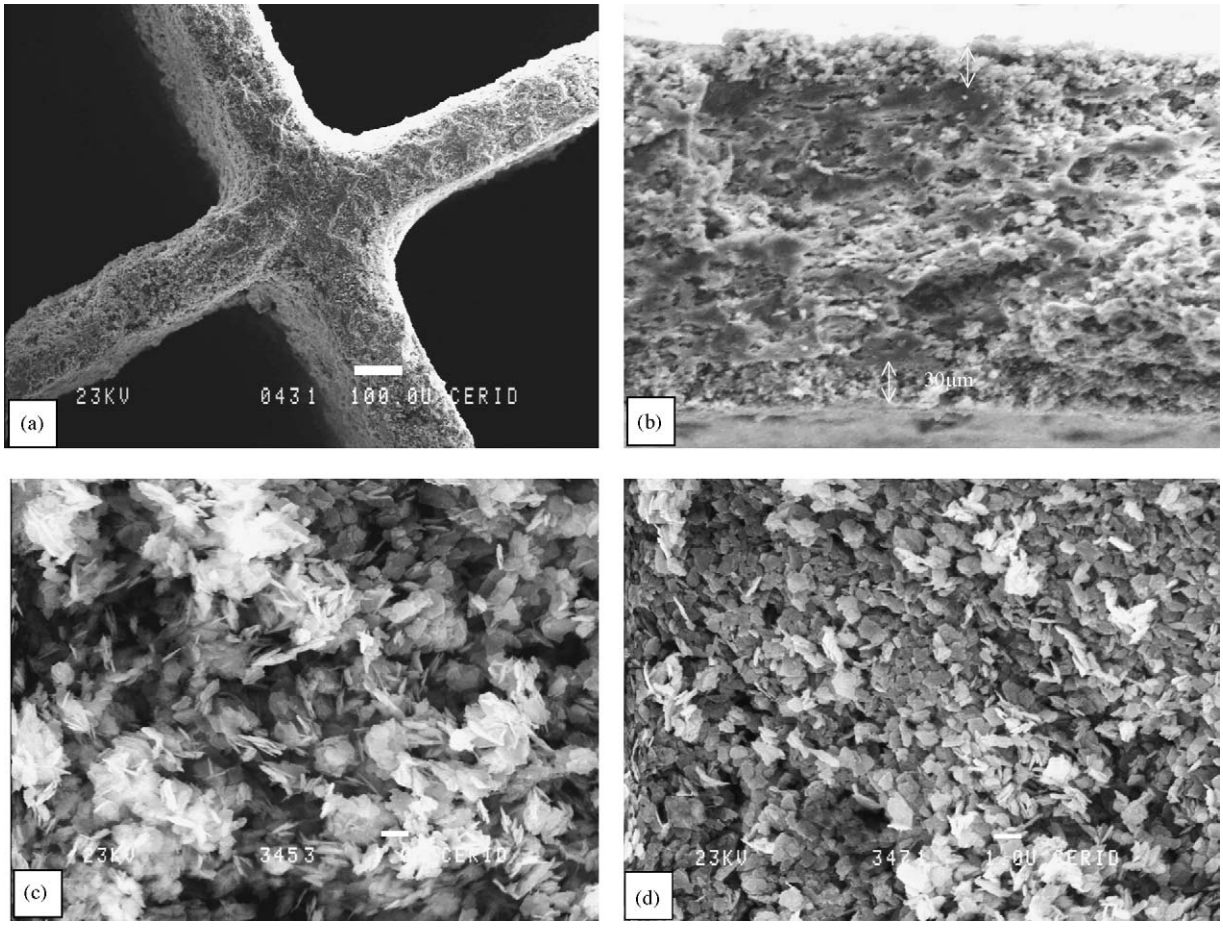

Fig. 6. SEM pictures of $PtCo_{3.4}$FER + SiO_2 coated on a cordierite monolith. (a) Front view of monolith walls, (b) transversal cut of a monolith piece, (c) details of calcined coating and (d) coating after use.

reported in the literature as the main observable species [19–22]. It is well known that Pt may also be in different forms inside the zeolite framework, mainly as exchanged ions and tiny metallic clusters. In a previous work [23], we concluded that in order to obtain an active, selective catalyst for the reduction of NO_x with methane in the presence of excess oxygen, a close interaction between Co and Pt is needed. Calcination and/or reduction between exchanges lead to preferential platinum expulsion from the zeolite lattice and the consequent drop in selectivity. On the other hand, the most selective catalysts contain Co^{2+} at exchange positions plus small clusters of cobalt and platinum oxides. The main causes of non-selectivity are the decreased concentration of Co^{2+} exchanged ions combined with Co_3O_4 and Pt clusters formation. The different steps necessary to obtain a PtCoFerrierite attached to a cordierite monolith may lead to non-selective catalysts, and the addition of 2% (w/w) of silica binder to the slurry helps maintain the good performance of the powder [16].

The variation of the Co/Pt ratio also modifies the catalytic behavior. As shown in Table 1, PtCoFER with Co/Pt = 30 is better than CoFER. However, with decreasing Co/Pt ratios, the performance gets worse to the point that for Co/Pt = 9.7 it becomes less selective than the monometallic ferrierite. Excess of Pt would result in the formation of Pt crystals on the outer surface of zeolite crystals, thus favoring the deep oxidation of methane.

In the case of non-Pt catalysts, the results also indicate the existence of an optimum Co loading at 1.2 wt% or lower. Similar to what happens with Pt, the formation of Co_3O_4 at higher loadings would be deleterious to selectivity. TPR and LRS characterization helps gain insight into these aspects. It is worth noticing that monoliths washcoated with PtCo-Ferrierite have the same performance as the starting powders. This is possible with the addition of the SiO_2 binder; without it, the catalyst becomes non-selective and only burns methane, as previously reported [16]. Note that since the monolithic catalyst is as good as the powder, there are no diffusive restrictions due to the coating thickness.

The TPR results shown in Fig. 3 are in line with the previous analysis. The presence of Co_3O_4 in the CoFerrierite with increasing loadings of Co is responsible for the lowering in selectivity for the NO_x reduction towards N_2. Moreover, after use under dry conditions, the amount of the non-selective oxide increases which indicates that not only is the Co_3O_4 present in the fresh sample important in the selectivity drop but also the Co species that are precursors of the formation of Co_3O_4 under reaction conditions. These precursors can be Co^{2+} exchanged ions that are expelled from exchange positions or non-crystalline well-dispersed Co oxide species that coalesce to form the more crystalline Co_3O_4, most probably on the outer surface of zeolite crystals. The Raman spectra help to better understand this phenomenon.

The solid with 1.2% Co could not be characterized using Raman due to its fluorescence. Anyway, from TPR results we can assert that the main Co species is exchanged Co^{2+} ions. In the samples with higher Co loading, the Raman signals corresponding to Co_3O_4 clearly increased after use but we were not able to detect the characteristic bands of non-crystalline Co oxides, which, as stated above, are probable precursors of the formation of well-defined oxide crystals. Thus, it is suggested that in CoFerrierite, Co^{2+} are expelled from exchange positions during their use under reaction conditions.

The Raman spectra of washcoated monoliths both with and without silica binder are in line with the above observations. Catalysts showing the characteristic Co_3O_4 signals are non-selective while those showing only non-crystalline Co oxide species have a good performance in NO_x reduction. These results are in line with our previous findings about the negative role of Co_3O_4 species. Laser Raman spectroscopy resulted a powerful tool to gain insight into the nature of non-selective Co species sitting on the ferrierite framework.

The XPS results shown in Table 2 help develop a more thorough description of the system under study. In the bimetallic catalyst with higher Co content ($PtCo_{4.3}FER$), the Co/Si ratio remains constant after use under reaction conditions, while the Pt/Si ratio decreases. This solid is the most selective one among those studied in this work. On the contrary, for the used catalyst with the lowest Co loading ($PtCo_{1.2}FER$) the Co/Si ratio strongly decreases and the Pt/Si ratio increases. After a treatment with 10% water in the feed the Co/Si ratio decreased 15 times and the Pt/Si ratio increased 5 times (bottom line in Table 3), and this catalyst is non-selective.

The binding energy and the FWHM of the Co $2p_{3/2}$ signal remain almost constant for all the samples (Table 3). This might indicate that the amount of Co_3O_4 formed is small compared to the Co^{2+} at exchange positions. Alternatively, this could be a consequence of higher exposure of Co^{2+} at the upper layers of the bimetallic zeolites. The variation in the Pt $4f_{3/2}$ binding energy is likely to be related to different sizes of the Pt crystals as reported by Vedrine et al. [18].

From the XPS and Raman information obtained two different mechanisms of deactivation must be operative in ferrierites with high and low Co loadings. For high loadings, the formation of Co_3O_4 is mainly responsible for the lack of selectivity, while for samples with low Co loadings, the formation of Pt clusters in the outer surface of zeolite crystals produces the said effect. Moreover, for the $PtCo_{1.2}FER$ sample, Co migrates inside the crystals, suggesting that reactants easily access the Pt particles, which are highly active for methane combustion with oxygen.

5. Conclusions

It has been shown that the selectivity of NO_x reduction can be optimised by adjusting the Co loading and the Co/Pt ratio in monometallic and bimetallic catalysts, respectively.

Thus, the adjustment of the metal composition becomes a key step in the preparation procedure.

Another important conclusion of this work concerns the deactivation mechanism in bimetallic catalysts (PtCoFER). For low Co loadings, the formation of Pt clusters at the outer-surface of ferrierite crystals, and the migration of Co to less accessible positions are the reasons for the selectivity drop. On the other hand, for higher Co loadings, the Co_3O_4 crystals probably also located outside the crystals are the non-selective species that only burn methane leaving unreacted NO_x molecules.

Finally, this work is an interesting example of the powerful combination of XPS and Raman techniques for catalyst characterization. They have provided data to prove the existence of two different deactivation mechanisms in the solids studied.

Acknowledgments

The authors wish to acknowledge the financial support received from UNL, CONICET and ANPCyT. They are also grateful to the Japan International Cooperation Agency (JICA) for the donation of the major instruments used in this study. Thanks are finally given to Prof. Elsa Grimaldi for the English language editing.

References

[1] R.M. Heck, R.J. Farrauto, Catalytic air pollution control, in: Commercial Technology, Van Nostrad Reinhold, New York, 1995.
[2] I-S. Nam, S.T. Choo, D.J. Koh, Y.G. Kim, Catal. Today 38 (1997) 181.
[3] H. Choi, S.-W. Ham, I.-S. Nam, Y.G. Kim, Ind. Eng. Chem. Res. 35 (1) (1996) 106.
[4] J.N. Armor, Catal. Today 26 (1995) 147.
[5] H. Hamada, Catal. Surv. Jpn. 1 (1997) 53.
[6] E. Kikuchi, M. Ogura, N. Aratani, Y. Sugiura, S. Hiramoto, K. Yogo, Catal. Today 27 (1996) 35.
[7] E. Kikuchi, M. Ogura, Catal. Surv. Jpn. 1 (1997) 227.
[8] M. Ogura, Y. Sugiura, M. Hayashi, E. Kikuchi, Catal. Lett. 42 (1996) 185.
[9] F. Bustamante, F. Córdoba, M. Yates, C. Montes, Appl. Catal. A: Gen. 234 (2002) 127.
[10] R. Heinisch, M. Jahn, C. Yalamas, Chem. Eng. Technol. 22 (1999) 4.
[11] M.A. Ulla, R. Mallada, J. Coronas, L. Gutierrez, E. Miró, J. Santamaría, Appl. Catal. A: Gen. 253 (1) (2003) 269.
[12] M.A. Ulla, E. Miró, R. Mallada, J. Coronas, J. Santamaría, Chem. Commun. (2004) 528.
[13] A.E.W. Beers, T.A. Nijhuis, F. Kapteijn, J.A. Moulijn, Micropor. Mesopor. Mater. 48 (2001) 279.
[14] C. Agrafiotis, A. Tsetsekou, A. Ekonomakou, J. Mater. Sci. Lett. 18 (1999) 1421.
[15] J.M. Zamaro, M.A. Ulla, E.E. Miró, Chem. Eng. J. 106 (2005) 25.
[16] A. Boix, J. Zamaro, E.A. Lombardo, E.E. Miró, Appl. Catal B: Env. 46 (2001) 121.
[17] M. Vuurman, D. Strufkens, A. Oskam, G. Deo, I. Wachs, J. Chem. Soc. Faraday Trans. 92 (1996) 3259.
[18] J.C. Vedrine, M. Dufaux, C. Naccache, B. Imelik, J. Chem. Soc. Faraday I 74 (1978) 440.
[19] J. Dedecek, D. Kaucký, B. Wichterlová, Micropor. Mesopor. Mater. 35–36 (2000) 483.
[20] D. Kaucký, A. Vondrová, J. Dedecek, B. Wichterlová, J. Catal. 194 (2000) 318.
[21] X. Wang, H. Chen, W.M.H. Sachtler, Appl. Catal. B: Environ. 29 (2001) 47.
[22] X. Wang, H. Chen, W.M.H. Sachtler, Appl. Catal. B: Environ. 26 (2000) 227.
[23] L. Gutierrez, A. Boix, E.A. Lombardo, J.L. García Fierro, J. Catal. 195 (2001) 60.